



POLİTEKNİK DERGİSİ

JOURNAL of POLYTECHNIC

ISSN: 1302-0900 (PRINT), ISSN: 2147-9429 (ONLINE)

URL: <http://dergipark.org.tr/politeknik>



Implementation of three phase induction motor pre-design program on electronic circuit

Elektronik devre üzerinde üç fazlı indüksiyon motor ön tasarım programının uygulanması

Yazar(lar) (Author(s)): Hasbi APAYDIN¹, Necibe Füsun OYMAN SERTELLER², Yüksel OĞUZ³

ORCID¹: 0000-0003-4500-2803

ORCID²: 0000-0003-3147-2740

ORCID³: 0000-0002-5233-151X

To cite to this article: Apaydın H., Necibe Füsun O. S. ve Oğuz Y., "Implementation of three phase induction motor pre-design program on electronic circuit", *Journal of Polytechnic*, *(*) : *, (*).

Bu makaleye şu şekilde atıfta bulunabilirsiniz: Apaydın H., Necibe Füsun O. S. ve Oğuz Y., "Implementation of three phase induction motor pre-design program on electronic circuit", *Politeknik Dergisi*, *(*) : *, (*).

Erişim linki (To link to this article): <http://dergipark.org.tr/politeknik/archive>

DOI: 10.2339/politeknik.1217145

Implementation of Three Phase Induction Motor Pre-Design Program on Electronic Circuit

Highlights

- ❖ *The analytical equations used in the preliminary design of the three-phase induction motor are discussed in detail.*
- ❖ *Studies on the calculations of the three-phase induction motor, whose analytical equations are considered, have been examined.*
- ❖ *Electronic circuit and software have been developed to be used in the preliminary design calculations of the three-phase induction motor.*
- ❖ *Calculations of a sample three-phase induction motor were made on the developed electronic circuit.*

Graphical Abstract

An electronic circuit consisting of a Nextion touchscreen and Arduino card has been developed to be used in the preliminary design calculations of the three-phase induction motor.



Figure. Application circuit consisting of Arduino Mega 2560 and Nextion 7-inch touch screen

Aim

The study aimed to develop an alternative to the programs used in the preliminary design of the three-phase induction motor by creating an induction motor pre-design calculation circuit and a program.

Design & Methodology

The electronic circuit was created using the Nextion 7-inch touch screen and Arduino Mega 2560. A program has been developed in which asynchronous motor preliminary design calculations can be made on the created circuit.

Originality

Being a portable three-phase induction motor pre-design calculation platform consisting of a touch screen.

Findings

The time spent on induction motor analytical calculations is huge. Calculation errors may occur due to the person performing the calculation. This study largely eliminates these negativities.

Conclusion

While various programming languages have been used to develop three-phase induction motor calculation programs, this study presents a portable analytical calculation tool for three-phase induction motors that operate independently of a computer environment. Mathematical calculations were conducted using sample motor parameters, and the results aligned with those obtained from the analytical calculation tool created.

Declaration of Ethical Standards

The authors of this article declare that the materials and methods used in this study do not require ethical committee permission and/or legal-special permission.

Implementation of Three Phase Induction Motor Pre-Design Program on Electronic Circuit

Araştırma Makalesi/Research Article

Hasbi APAYDIN^{1*}, Necibe Füsün OYMAN SERTELLER¹, Yüksel OĞUZ²

¹ Faculty of Technology, Electrical and Electronics Engineering, Marmara University, Istanbul, Turkey

² Faculty of Technology, Electrical and Electronics Engineering Afyon Kocatepe University, Afyonkarahisar, Turkey
(Geliş/Received : 10.12.2022 ; Kabul/Accepted : 28.05.2023 ; Erken Görünüm/Early View : 14.06.2023)

ABSTRACT

In this study, the performance analysis of a 5.5 kW, 460 V, 60 Hz, 4-pole, and 3-phase squirrel-cage induction motor (IM) has been carried out by developing a portable electronic circuit, design, and the software, independent of any commercial software. The mathematical equations used in the design steps and the preliminary design of the main dimensions of the squirrel-cage IM are realized with a developed electronic circuit. To perform preliminary design calculations Nextion 7-inch touch screen, Arduino mega 2560 microcontroller is used in electronic circuit design. Briefly, IM basic data are entered from the Nextion 7 inches touch screen in the electronic circuit created and the data are sent to the Arduino Mega 2560 microcontroller card via serial communication. On the Arduino Mega 2560 microcontroller board, IM mathematical calculations are accomplished, and the calculation results are presented on the Nextion screen. It has been observed that the analytical calculations and the calculation results in the developed calculation tool have been obtained in good agreement.

Keywords: Electrical machine design tools, induction motor prototype design, motor design software, Nextion touch screen, Arduino.

Elektronik Devre Üzerinde Üç Fazlı İndüksiyon Motor Ön Tasarım Programının Uygulanması

ÖZ

Bu çalışmada, herhangi bir ticari yazılımdan bağımsız taşınabilir elektronik devre, tasarım ve yazılım geliştirilerek 5,5 kW, 460 V, 60 Hz, 4 kutuplu ve 3 fazlı sincap kafesli indüksiyon motorun (İM) performans analizi yapılmıştır. Sincap kafesli İM'nin tasarım adımlarında kullanılan matematiksel denklemler ve ana boyutlarının ön tasarımı, geliştirilen bir elektronik devre ile gerçekleştirilmiştir. Ön tasarım hesaplamalarının yapılabilmesi için Nextion 7 inçlik dokunmatik ekran, elektronik devre tasarımında Arduino mega 2560 mikrodeneleyici kullanılmıştır. Kısaca oluşturulan elektronik devrede Nextion 7 inçlik dokunmatik ekrandan İM temel verileri girilir ve veriler Arduino Mega 2560 mikrodeneleyici kartına seri haberleşme ile gönderilir. Arduino Mega 2560 mikrodeneleyici kartı üzerinde İM'nin matematiksel hesaplamaları yapılır ve hesaplama sonuçları Nextion ekranında sunulur. Geliştirilen hesaplama aracında yapılan analitik hesaplamalar ile hesaplama sonuçlarının uyumlu bir şekilde elde edildiği görülmüştür.

Anahtar Kelimeler: Elektrikli makine tasarım araçları, indüksiyon motoru prototip tasarımı, motor tasarım yazılımı, Nextion dokunmatik ekran, Arduino.

1. INTRODUCTION

Induction motors (IMs) are electric motors commonly used in industry. The main reasons for their widespread usage are that they are cheaper than other electrical machines and require less maintenance [1-3]. While IMs are so widely used, the slightest increase in efficiency in these motors can reduce a large amount of energy consumption worldwide [4,5]. Therefore, electrical machines' efficient preliminary design is of vital importance. With the improvement of computer software technology the virtual platforms created for the design of electrical machines, have been started to be utilized more. [6]. The most efficient, appropriate dimensions and high standards pre-design is being carried out visual platform, before IM's production [7]. By using computer-based

software, users can instantly observe the effect of motor parameters on efficiency and motor size and analyze machine performance. Users and manufacturers can choose the optimum motor design among the models they create [8]. There is commercial software available in the market serving this purpose, as well as software developed by academic studies. When the literature is scanned, the studies on IM preliminary design are as follows. Scutaru and his colleagues have created a visual program in which they can design a 3-phase IM using the visual basic software language. In the visual program, the user manually enters the stator, rotor geometric parameters, and input parameters into the program and the output parameters of the motor can be examined by the program [9]. Aravind and his colleagues have stated that the design of electrical machines, in general, is complex. Based on the statement, they have created a

*Sorumlu Yazar (Corresponding Author)
e-posta : hasbiapaydin@marun.edu.tr

simple and understandable design tool. They created their design tool by using Matlab/GUI and created an interface that performs IM, direct current motor, synchronous motor and switched reluctance motor design. They have successfully designed electrical machines [10]. Bhaskar created a model for obtaining IM-appropriate dimensions using Matlab/SIMULINK. Different examples are considered to test the success of the software [11]. Aguiar and his colleagues have developed a computer-aided tool for 3-phase IM design. They express that it will bring flexibility for motor design engineers. The user interface is built using Matlab/GUI. It is aimed to contribute to the high-efficiency design of Brazilian standard motors. They observe that it is effective as the first step in machine design by changing the parameters of the program without the requirement for any other tool [12]. Zöhra and Akar, an interface program with a power of 5.5 kW was designed in accordance with IM standards, which were dimensioned geometrically, electrically, and magnetically. In the interface design, Matlab-GUI is used. Motor performance graphs are obtained through the developed interface program and studies are carried out to improve the design parameters. The performance of the interface program has been tested by comparing it with industrial products and the design data obtained from the design program within the scope of the study [13]. Deepa and Bindu's work presents a software development for the design of a three-phase IM on the computer environment. Visual Basic 6 and Microsoft Excel software were used. It was developed in Microsoft Access, which contains information about the standards and material properties used to manufacture the motor. The aim of this software is to reduce redesign time while learning the IM design procedure. The software allows user to verify their designs and analyze the performance of the machine by modifying the related parameters in less time [14]. Ike et al., a computer program was developed in Matlab programming and applied for the program they developed for the renewal of a faulty IM. They carried out the practical calculations of 3-phase 48-slot squirrel-cage IM and the design of the stator winding. The stator winding was tested by rewinding using the program result data. As a result of the test, they stated that the performance was good in the unloaded test result and that no heating occurred in the motor [15]. Somashekar created a calculation tool consisting of codes in the Matlab program in order to make this process faster and error-free, starting from the time-consuming and complex nature of IM calculations. He stated that it would provide support to students who have an IM course in their curriculum during the IM design process [16].

The IM preliminary design application circuit, which deals with and solves the IM design with analytical equations in detail, has been prepared in this study. A user interface has been developed where the rotor, stator, electrical and magnetic parameters of the IM can be entered on the portable Nextion 7-inch touch screen on the circuit. On the User Interface screen, the parameters

used in the design of the IM have been arranged and made simpler and more understandable. Serial communication is provided with the Arduino Mega 2560 so that mathematical calculations can be made by the users depending on the motor parameters entered in the relevant places on the user interface. Mathematical calculations have been realized on the Arduino Mega card and the calculated data are transferred to the user interface created on the Nextion screen. Users can perform IM main dimensions, stator-rotor physical dimensions, stator-rotor electrical calculations, and stator-rotor loss calculations, depending on design criteria which they defined using the IM design platform and performance values.

2. DESIGN METHODOLOGY FOR INDUCTION MOTOR

The design equations in this section are provided from the references in [17-22]. The apparent airgap power

$$S_{gap} \text{ (VA)} = \frac{K_E \cdot P_n}{\eta_n \cdot \cos \phi_n} \quad (1)$$

P_n (Watt), η_n , $\cos \phi_n$, and K_E are output power, efficiency, power factor, and voltage drop coefficient respectively. K_E is approximately given in equation (2):

$$K_E \cong 0.98 - 0.005 \cdot p \quad (2)$$

Expressions given in equations is the $2p$ total pole numbers. Armature diameter D_{is} (m) is

$$D_{is} = \sqrt[3]{\frac{2p \cdot p \cdot S_{gap}}{\pi \cdot \lambda \cdot F \cdot C_0}} \quad (3)$$

Expressions given in equations is F (Hz) frequency, λ the stack length to pole pitch ratio, and C_0 volume utilization factor (Esson's constant). C_0 value is given in Figure 1 depending on S_{gap} and p .

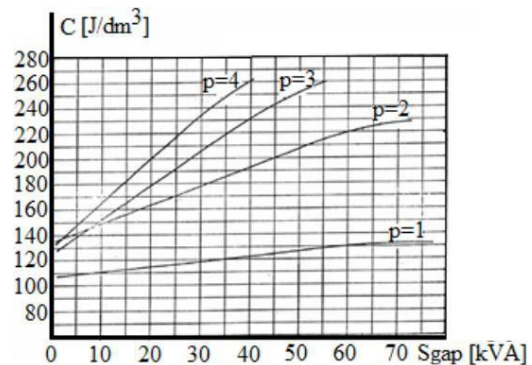


Figure 1. Esson's constant C_0 versus S_{gap} [17]

Length to pole pitch ratio λ , pole pitch tp (m), and slot pitch ts (m) are given in equation (4):

$$tp = \frac{\pi \cdot D_{is}}{p}, \quad \lambda = \frac{L}{tp}, \quad ts = \frac{tp}{3 \cdot q} \quad (4)$$

Expressions given in equations is L (m) stator bore length. λ is 1.5 for high efficiency [17]. The air gap length g (m) is calculated as in Equation (5).

$$g = \left(0.1 + 0.02 \cdot \sqrt[3]{P_n}\right) \cdot 10^{-3} \text{ for } 2p = 2 \quad (5)$$

$$g = \left(0.1 + 0.012 \cdot \sqrt[3]{P_n}\right) \cdot 10^{-3} \text{ for } 2p > 2$$

Pol flux \tilde{f}_i (Wb) and the number of turns per phase $W1$ (turns/phase) are given equationstions (6) and (7):

$$\tilde{f}_i = \alpha_i \cdot tp \cdot L \cdot B_g \quad (6)$$

$$W1 = \frac{K_E \cdot V_{ph}}{4 \cdot k_f \cdot K_{w1} \cdot F \cdot \tilde{f}_i} \quad (7)$$

The airgap flux density B_g (T) value is in the (0.5 - 0.75) T range for $2p = 2$, the (0.65 - 0.78) T range for $2p = 4$, the (0.7 - 0.82) T range for $2p = 6$, and the (0.75 - 0.85) T range for $2p = 8$. K_{w1} is stator winding factor. V_{ph} is phase voltage. Flux density shape factor α_i and form factor k_f depends of the tooth saturation factor $1 + k_{st}$. The α_i and k_f value are found using Figure 2 based on the $1 + k_{sd}$

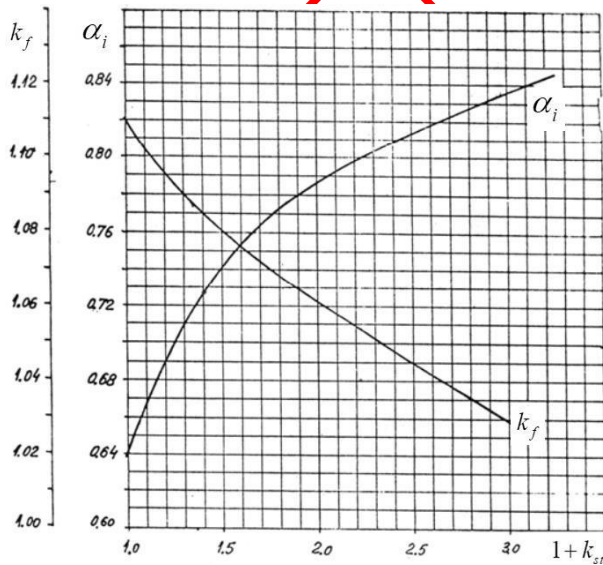


Figure 2. Flux density shape factor α_i and form factor k_f versus tooth saturation factor [17]

Rated current I_{1n} (A), magnetic wire cross section A_{C0} (mm^2), and wire gauge diameter d_{C0} (mm) are given in equation (8), (9), and (10):

$$I_{1n} = \frac{P_n}{\sqrt{3} \cdot V \cdot \eta_n \cdot \cos \varphi_n} \quad (8)$$

$$A_{C0} = \frac{I_{1n}}{J_s} \quad (9)$$

$$d_{C0} = \sqrt{\frac{4 \cdot A_{C0}}{\pi}} \quad (10)$$

J_s (A/mm^2) in the equations is the stator current density. Suggested current densities: (4 - 7) A/mm^2 for $2p = 2, 4$ and (5 - 8) A/mm^2 for $2p = 6, 8$.

Before stator and rotor slot designs are performed, the main dimensions are determined. Stator and rotor geometries in Figure 3 were used for these designs.

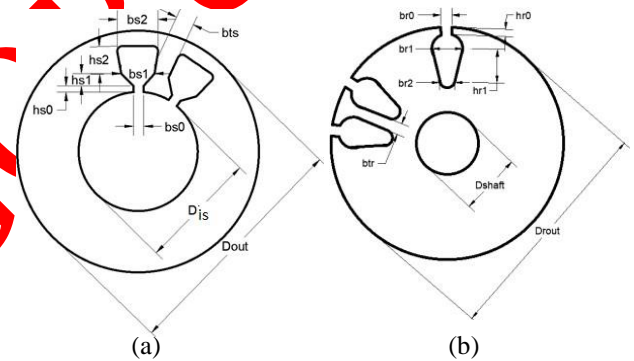


Figure 3. Stator geometry (a) and rotor geometry (b)

The stator useful slot area can be calculated in equation (11):

$$A_{ts} = \frac{\pi \cdot d_{C0}^2 \cdot ap \cdot ns}{4 \cdot K_{fill}} \quad (11)$$

K_{fill} in the equations is slot fill factor. K_{fill} is in the range of approximately 0,35 to 0,4 below 10 kW and 0.4 to 0.44 above 10 kW. ns and ap are the number of turns per slot and the number of conductors in parallel, respectively. If we accept all the air gap flux passes through the stator teeth., equality (12) can be written:

$$B_g \cdot L \cdot ts \cong B_{ts} \cdot L \cdot b_{ts} \cdot K_{FE} \quad (12)$$

The tooth flux density B_{ts} (T) value is in the (1.5 - 1.65)T range. K_{FE} is the stacking factor. The stator slot teeth

width b_{ts} (m) can be written as equation (13) using equation (12).

$$b_{ts} \cong \frac{B_g \cdot ts}{B_{ts} \cdot K_{FE}} \quad (13)$$

Upper diameter of stator slot b_{s1} (m), lower diameter of stator slot b_{s2} (m), and stator slot height h_{s2} (m) are given in equation 14.

$$b_{s1} = \frac{\pi \cdot (D_{is} + 2 \cdot h_{s0} + 2 \cdot h_{s1})}{N_s} - b_{ts},$$

$$b_{s2} = \sqrt{4 \cdot A_{us} \cdot \tan\left(\frac{\pi}{N_s}\right) - b_{s1}^2}, h_{s2} = \frac{4 \cdot A_{us}}{b_{s1} + b_{s2}} \quad (14)$$

The airgap mmf (magnetomotive force) F_{mg} (A-turns) and the stator tooth mmf F_{mst} (A-turns) is given in equation (15).

$$F_{mg} \cong 1.2 \cdot g \cdot \frac{B_g}{\mu_0}, \quad F_{mst} = H_{ts} \cdot (h_{s0} + h_{s1} + h_{s2}) \quad (15)$$

μ_0 (H/m) in equation (15) is the permeability of free space and the H_{ts} (A/m) value is found according to the B_{ts} value by using the magnetization curve. The rotor tooth mmf F_{mtr} value is calculated depending on the tooth saturation factor $(1 + k_{sat})$ as in equation (16).

$$F_{mtr} = K_{st} \cdot F_{mg} - F_{mst} \quad (16)$$

The F_{mtr} value should be approximately equal to the F_{mst} value. If this procedure is not provided recalculations should be made by changing the value of $1 + k_{sat}$.

Before we can calculate the rotor slot area A_b and the end ring cross section A_{er} , we need to calculate the rotor bar current I_b (A) and the end ring current I_{er} (A). I_b , I_{er} , A_b , and A_{er} are given in equation (17). The J_b (A/mm^2) value in equation (17) is the rotor bar current density, the J_{er} (A/mm^2) value is the end ring current density, and the N_r value are the number of rotor slots.

$$I_b = \frac{8}{10} \cdot \cos \varphi_n \cdot \frac{2 \cdot m \cdot W1 \cdot K_{wl}}{N_r} \cdot I_{1n}, \quad A_b = \frac{I_b}{J_b},$$

$$I_{er} = \frac{I_b}{2 \cdot \sin\left(\frac{\pi \cdot p}{N_r}\right)}, \quad A_{er} = \frac{I_{er}}{J_{er}} \quad (17)$$

The rotor slot pitch tsr (m) and the rotor tooth width b_{tr} (m) are given in equation (18).

$$tsr = \frac{\pi \cdot D_{roul}}{N_r}, \quad b_{tr} = \frac{B_g \cdot tsr}{B_{tr} \cdot K_{FE}} \quad (18)$$

Upper diameter of rotor slot b_{r1} (m), lower diameter of rotor slot b_{r2} (m), and rotor slot height h_{r1} (m) are given in equation (19).

$$b_{r1} = \frac{\pi \cdot (D_r - 2 \cdot h_{r0}) - N_r \cdot b_{tr}}{\pi + N_r},$$

$$b_{r2} = \sqrt{\frac{8 \cdot A_b \cdot \tan\left(\frac{\pi}{N_r}\right) - b_{r1}^2 \cdot (\pi \cdot \tan\left(\frac{\pi}{N_r}\right) + 2)}{\pi \cdot \tan\left(\frac{\pi}{N_r}\right) - 2}},$$

$$h_{r1} = \frac{b_{r1} - b_{r2}}{\pi \cdot \tan\left(\frac{\pi}{N_r}\right)} \quad (19)$$

Equations (1)-(19) have been used to determine the main dimensions of the IM, the stator, and the rotor geometric dimensions. After dimensioning the IM, magnetization current, resistances-inductances, and losses-efficiency calculations have been found using the equations in reference [17].

3. MATERIAL METHOD

In order to make data entry easy and to see the calculation results in the system where the calculations of the three-phase IM can be performed, Nextion 7 inch touch screen has been chosen. Nextion display modules offer a unique Human Machine Interface (HMI) solution that acts as a modern interface for both control and display purposes such as LCD. It is the product of ITEAD company, has an editor for the development of programs, and editor allows the editing of the properties of each object. In this respect, it differs from conventional LCD displays. It acts as a stand-alone computer with a screen thanks to its built-in controller. By designing the screen such as button, label, graphic area, picture with the Nextion editor installed on the computer, a .tft file can be uploaded to the SD card and transferred to the screen. Nextion displays have a serial port that can communicate with the Arduino [23,24].

To process the parameters of the IM coming from the Nextion screen, Arduino Mega 2560 microcontroller is preferred because it is a useful, flexible, and open-source electronic circuit development platform with a microcontroller in its structure. Arduino Mega is a board containing an Atmega 2560 microcontroller with a frequency of 16 Mhz as a microcontroller. The number of digital input and output pins is 54, 14 of which have PWM capability. Microcontroller programming on the Arduino mega board can be done with both USB and ICSP connectors [25,26]. Arduino Mega 2560 and Nextion 7 inches display connection diagram is shown in Figure 4 and the application circuit is shown in Figure 5.

The data on the graphical interface screen created on the Nextion screen is sent to the Arduino Mega microcontroller via serial communication and calculations are realized on the Arduino mega. The calculations realized on the Arduino Mega are then sent to the Nextion screen and displayed on the analysis result screens on the graphical interface screen.

Arduino, microcontroller, and STM cards (microcontrollers using ARM-based processors) can be used by communicating easily with Nextion screens and the interfaces that are developed through the application called Nextion Editor. The Nextion editor screenshot of the designed program is shown in Figure 6. The only

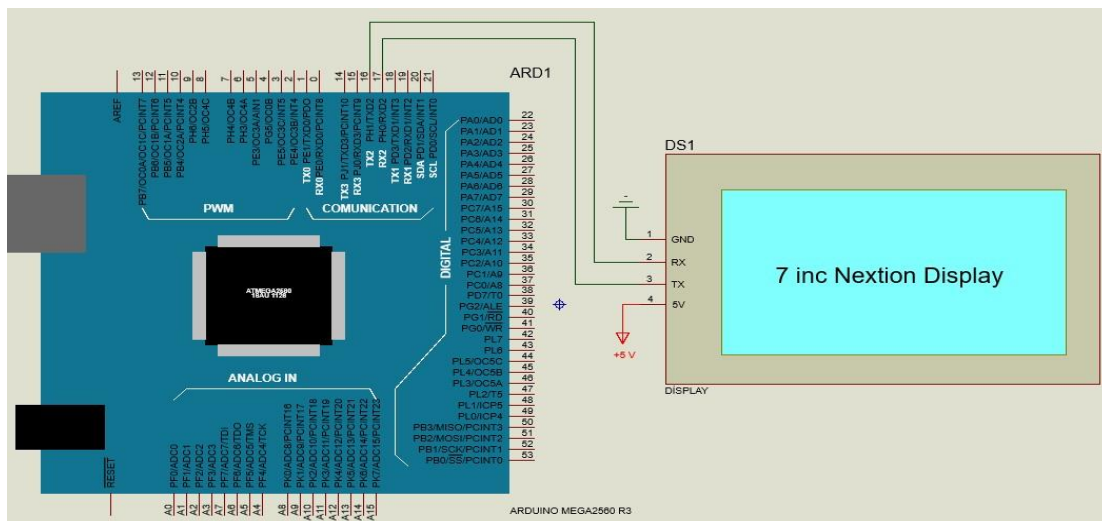


Figure 4. Connection schema with the devices Arduino mega and Nextion display



Figure 5. Application circuit consisting of Arduino mega and Nextion screen



Figure 6. ITEAD Nextion screen editor with the project

requirement for the Microcontroller to be used to communicate with the Nextion display is the Universal Asynchronous Transceiver (UART) interface. Nextion displays can communicate with the microcontrollers or microprocessors to be used via Universal Asynchronous Receiver Transmitter (UART) [27]. You can change the values on the Nextion screen by sending data over the UART line, or you can detect the touches via UART when you touch the Nextion screen. In addition, Isis electronic circuit design program was used for the simulation. The virtual instrumentation feature of the Isis program offers a great platform for simulation [28]. Thanks to the Isis program, it is possible to make simulations between the interface program created on the Nextion Editor in the computer environment, thus providing an advantage to the software development stage.

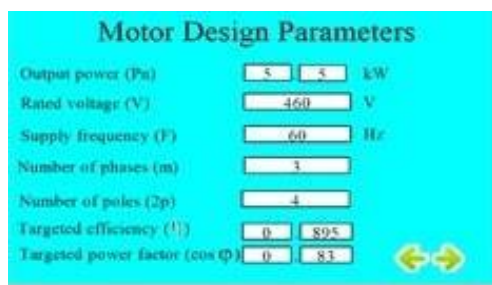
When the start button on the main screen is pressed, the first screen view welcomes us is the window where motor parameters are loaded. On this window, users must load the parameters of motor output power, rated voltage, supply frequency, number of phases, number of poles, targeted efficiency, and targeted power factor. This design screen is shown in Figure 7.

After loading the motor parameters, the next window is accessed by pressing the forward button. Users can enter the stator parameters from the page screen where the stator parameters are entered in the next page, Figure 8. On this screen, users must enter the stator slot number, stator current density, airgap flux density, stator tooth flux density, tooth saturation factor, and stacking factor values.

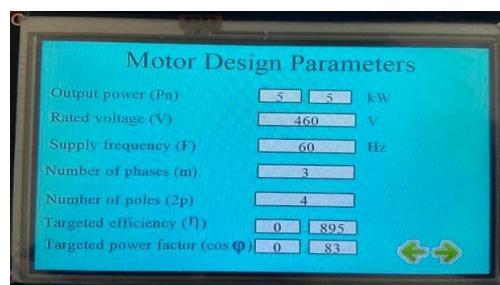
After loading the stator parameters, the next window is appeared by pressing the forward button. In the next

Table 1. Three-phase IM specifications [17].

Motor Parameters	Symbols/Units	Values	Motor Parameters	Symbols/Units	Values
Rated output power	$P_n(kW)$	5.5	$bs_0(mm)$		2.2
Rated voltage	$V(Volt)$	460	$hs_0(mm)$		1.0
Supply frequency	$F(Hz)$	60	$hs_1(mm)$		1.5
Number of phases	m	3	Number of rotor slots	N_r	28
Number of poles	$2p$	4	Number of rotor bars per slot	Z_{sr}	1
Targeted efficiency	η	0.895	Current density of rotor	$J_b(A/mm^2)$	3.42
Targeted power factor	$\cos \phi$	0.83	Flux density of rotor tooth	$B_r(T)$	1.60
Number of stator slot	N_s	36	Flux density of rotor back core	$B_{cr}(T)$	1.60
Current density of stator	$J_s(A/mm^2)$	4.50	Current density of end rings	$J_{er}(A/mm^2)$	0.75* J_b
Flux density of airgap	$B_g(T)$	0.70		$br_0(mm)$	1.5
Flux density of stator tooth	$B_{ts}(T)$	1.55		$hr_0(mm)$	1.5
Initial tooth saturation factor	$1+k_{st}$	1.40	Copper resistivity at 20°C.	$(\rho_{co})_{20^\circ C}(\Omega m)$	$1.78*10^{-8}$
Rotor/stator stacking factor	K_{FE}	0.96	Copper resistivity at 80°C.	$(\rho_{co})_{80^\circ C}(\Omega m)$	$2.17*10^{-8}$
Weight of iron per unit volume	$\gamma_{irone}(kg/m^3)$	7800	Resistivity of aluminum at 20°C.	$(\rho_{AL})_{20^\circ C}(\Omega m)$	$3.1*10^{-8}$
The specific losses for 1.0 T at 50 Hz	$p_{10}(W/kg)$	2			



(a)



(b)

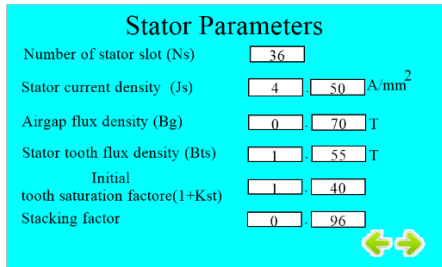
Figure 7. Nextion screen editor screen view of motor design parameters (a) and application circuit screen view of motor design parameters (b)

The parameters of the IM seen in Table 1 are entered using the Motor design parameters screen, Stator parameters screen, Stator slot geometry screen, Rotor parameters screen, and Rotor slot screen which are shown in Figure 7, 8, 9, 10, and 11 respectively.

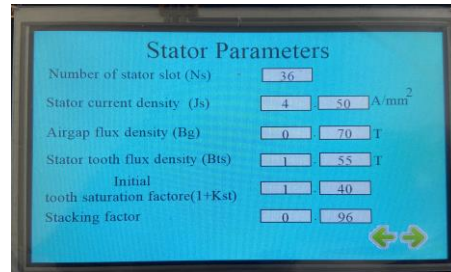
page, Figure 9, users can load the stator slot parameters from the window where rotor parameters are loaded. On this screen, users must enter the values of bs_0 , bs_1 , and hs_1 values.

After loading the stator slot geometry parameters, the next window is appeared by pressing the forward button. In the next page, Figure 10, users can load the rotor parameters from the window where rotor parameters are inputted.

After loading the rotor parameters, the next window is appeared by pressing the forward button. In the next window, in Figure 11, users can load the rotor slot parameters from the window where rotor slot parameters are loaded. On this screen, users are required to enter the values of br0 and hr0.

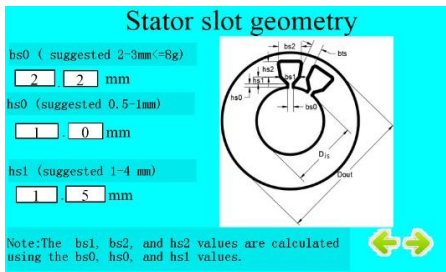


(a)

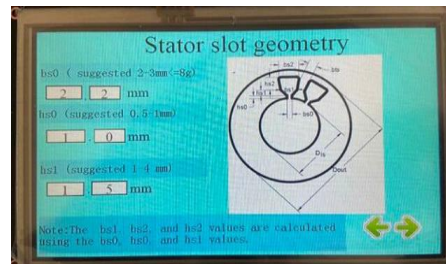


(b)

Figure 8. Nextion screen editor screen view of Stator parameters (a) and application circuit screen view of stator parameters (b)

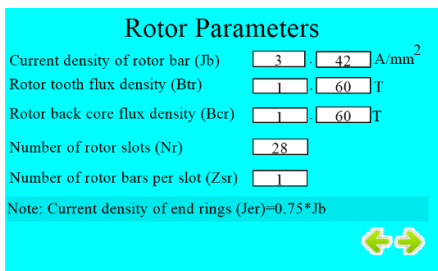


(a)

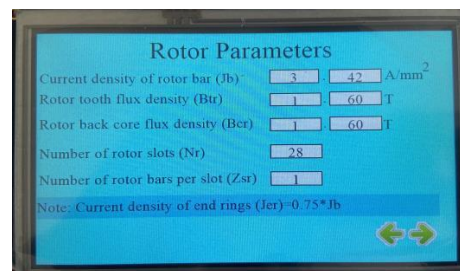


(b)

Figure 9. Nextion screen editor screen view of stator slot geometry parameters (a) and application circuit screen view of stator slot geometry parameters (b)

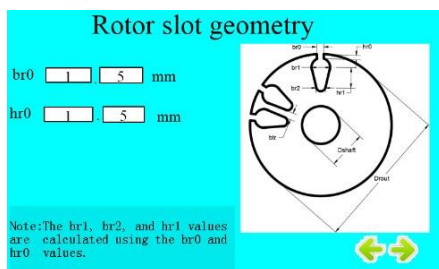


(a)

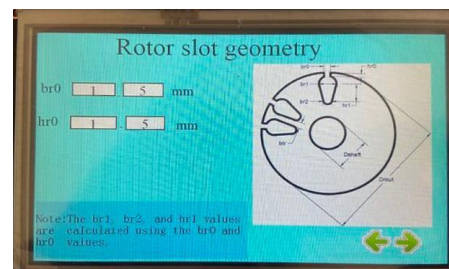


(b)

Figure 10. Nextion screen editor screen view of rotor parameters (a) and application circuit screen view of rotor parameters (b)



(a)



(b)

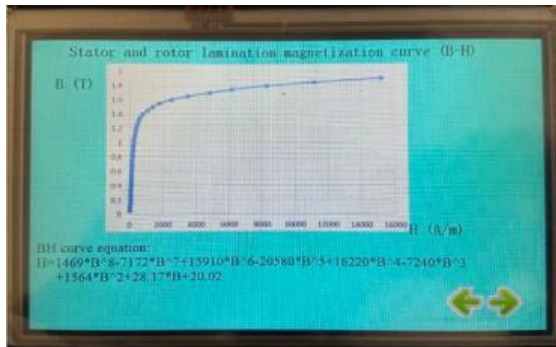
Figure 11. Nextion screen editor screen view of rotor slot geometry (a) and application circuit screen view of rotor slot geometry (b)

After the rotor slot parameters are loaded, the next windows are displayed when the next button is pressed sequentially. These windows: Stator and rotor lamination magnetization curve and BH curve equation, Esson's constand C_0 value versus S_{gap} and curve equations, and form factor and flux density shape factor versus tooth saturation and curve equation screen. Screen views are shown in Figure 12. Mathematical equations in the screen views in Figure 12 were created by curve fitting in the Matlab program, using the graphic data in the Figures.

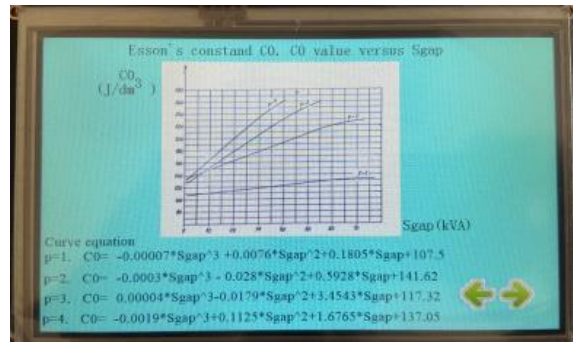
These equations were used by coding in the Arduino software.

The next windows appear by pressing the next button. These windows are check screen and analysis screen respectively. Screen views are shown in Figure 13.

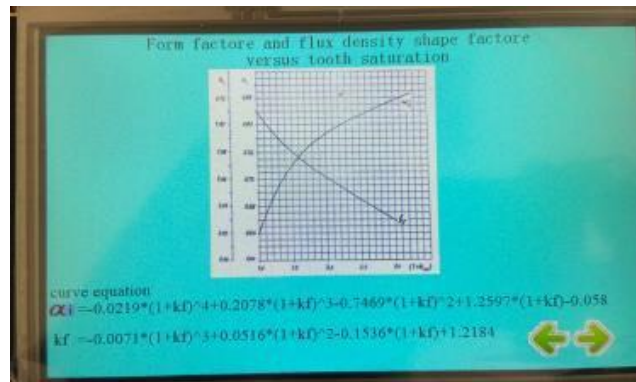
After pressing the Analyze button, the motor calculations are displayed on the screens. Screenshots of the analysis results can be seen in Figures 14, 15, and 16, respectively.



(a)

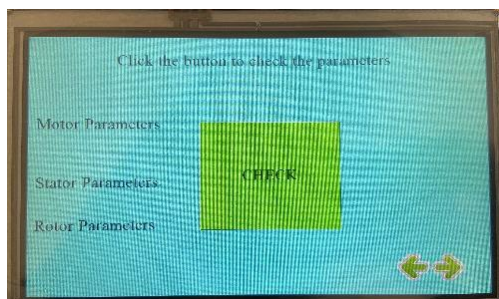


(b)

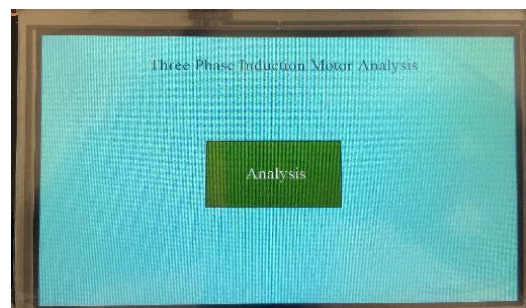


(c)

Figure 12. Application circuit screen view of stator and rotor lamination magnetization (B-H) (a), Esson's constand C_0 value versus S_{gap} (b), and form factor and flux density shape factor versus tooth saturation(c)

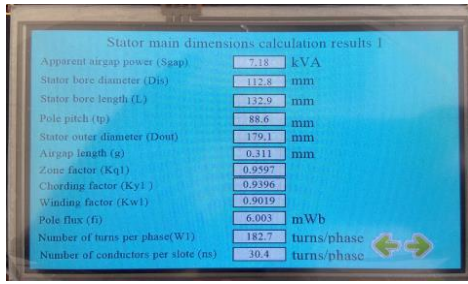


(a)

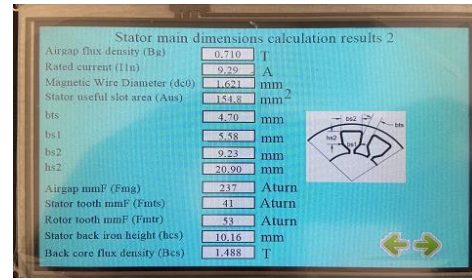


(b)

Figure 13. Application circuit screen view of check the parameters screen (a) and analysis screen (a)

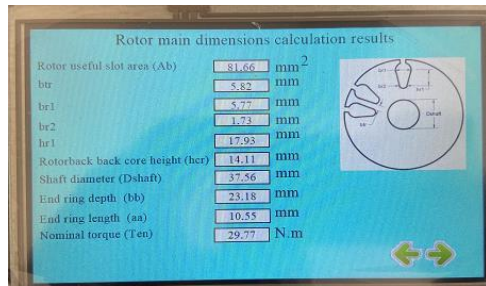


(a)

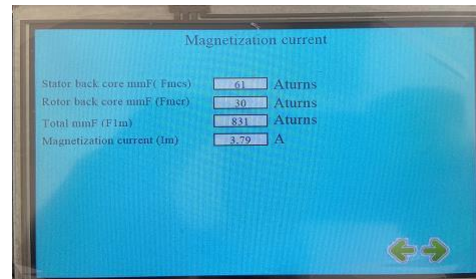


(b)

Figure 14. Application circuit screen view of stator main dimensions calculation results 1 (a) and stator main dimensions calculation results 2 (b)

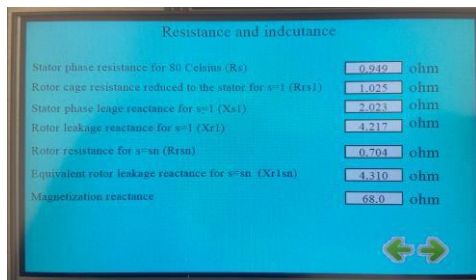


(a)

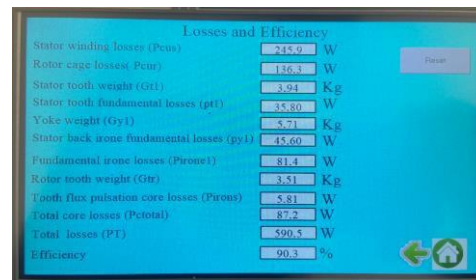


(b)

Figure 15. Application circuit screen view of rotor main dimensions calculation results (a) and magnetization current (b)



(a)



(b)

Figure 16. Application circuit screen view of resistance and inductance (a) and losses and efficiency (b)

Users can return to the main screen in Figure 9 by pressing the reset button on the losses and efficiency screen and selecting the home icon. They can change the parameters they want by using the screens where the related parameter is found. They can start the analysis and examine the analysis results according to the new parameters they have created. If the targeted efficiency cannot be reached, the actions to be taken can be listed as follows; is to reducing the stator or rotor current density and increasing the stator bore diameter or stack length.

4. FINDINGS AND DISCUSSION

Within the scope of this study, the calculations in the preliminary design of IM are carried out over the electrical-electronic circuit and the use of open-source code software in the electrical-electronic circuit has eliminated the software cost. It can be said that the

designing study is helpful, as the screen design on the circuit has an easy, accessible, and user-friendly interface to use. It allows users to enter data in a short time and, depending on the entered data, calculations can be made quickly with a single click. The desired changes on the data can be made easily, allowing the calculations to be performed over and over again. The flow chart is given in Figure 17.

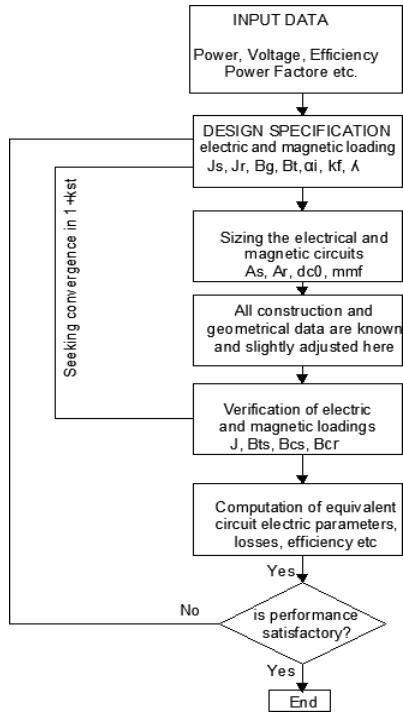


Figure 17. IM design procedure flow chart [17]

The analytical calculations made using the 3-phase IM parameters in Table 1 and the calculation results found in the work in references 17 and 29 are given in Table 2. As it is seen in Table 2, the results calculated in the preliminary design program and the analytical calculation results are found very close. The small difference values that occur are due to the determination coefficients of the equations created for the B-H curve, form factor, and flux density shape factor values used in the study.

MINIMUM

Table 2. Analytical calculation results of 3-phase IM and preliminary design program calculation results.

Motor Parameters	Variables	Unit	Reference Values [17]	Reference Values[29]	Obtained Values
Apparent Airgap Power	S_{gap}	kVA	7.1818	7.1818	7.18
Stator Bore Diameter	D_{is}	mm	111.60	111.40	112.8
Stack Length	L	mm	131.50	131.24	132.9
Pole Pitch	tp	mm	87.600	87.491	88.6
Stator Outer Diameter	D_{out}	mm	180.00	179.67	179.1
Airgap Length	g	mm	0.3111	0.3118	0.311
Zone Factor	K_{q1}		0.9598	0.9598	0.9597
Chording Factor	K_{y1}		0.9397	0.9397	0.9396
Stator Winding Factor	K_{w1}		0.9019	0.9019	0.9019
Pole Flux	fi	mWb	5.878	5.8592	6.003
Number Of Turns Per Phase	$W1$	turns / phase	186.80	187.21	182.7
Number Of Conductors Per Slot	ns	turns / slot	31.33	31.2	30.4
Airgap Flux Density	B_g	T	0.726	0.728	0.710
Rated Current	I_{ln}	A	9.303	9.2927	9.29
Magnetic Wire Diameter	d_{c0}	mm	1.622	1.6215	1.621
Stator Slot Sizing					
Useful Slot Area	A_{us}	mm ²	155.7	154.88	154.8
Stator Tooth Width	b_{is}	mm	4.75	4.7563	4.70
Stator Slot Lower Width	b_{s1}	mm	5.42	5.4012	5.58
Stator Slot Upper Width	b_{s2}	mm	9.16	9.1309	9.23
Stator Slot Useful Height	b_{s2}	mm	21.36	21.315	20.90
Mmf of Airgap	F_{mg}	Aturns	242.77	243.45	237
Mmf of Stator Tooth	F_{ms}	Aturns	41.99	41.915	41
Mmf of Rotor Tooth	F_{mr}	Aturns	55.11	55.465	53
Iron Height of Stator Back	h_{cs}	mm	10.34	10.322	10.16
Flux Density of Back Core	B_{cs}	T	1.456	1.4549	1.488
Rotor Slots Sizing					
Rotor Slot Area	A_b	mm ²	81.65	81.67	81.66

Table 2.(continue) Analytical calculation results of 3-phase IM and preliminary design program calculation results.

Rotor Tooth Width	b_{tr}	mm	5.88	5.8909	5.82
Upper Width of Rotor Slot	b_{r1}	mm	5.70	5.7696	5.77
Lower Width of Rotor Slot	b_{r2}	mm	1.200	1.697	1.73
Slot Height of Rotor	h_{r1}	mm	20.00	18.07	17.93
Rotor Back Core Height	h_{cr}	mm	13.55	13.529	14.11
Shaft Diameter	D_{shaft}	mm	35.90	39.032	37.56
Nominal Torque	T_{en}	Nm	29.77	29.774	29.77
End Ring Depth	bb	mm	24.445	24.533	23.18
End Ring Length	aa	mm	10.02	9.9734	10.55
Magnetization Current					
Mmf of Stator Back Core	F_{mcs}	Aturns	54.22	57.8030	61
Mmf of Rotor Back Core	F_{mcr}	Aturns	30.25	42.303	30
Total mmf	F_{lm}	Aturns	858,74	880.67	831
Magnetization Current	I_m	A	3.91	4.0169	3.79
Resistances and Inductances					
Phase Resistance of Stator at 80°C.	R_s	Ω	0.9367	0.4681	0.949
Reduced Rotor Cage Resistance to the stator	$RrSl$	Ω	1.1295	1.1512	1.025
Stator Phase Leakage Reactance	$Xs1$	Ω	2.1700	2.1937	2.023
Rotor Leakage Reactance	$Xr1$	Ω	3.6506	3.6284	4.217
Rotor Resistance	$RrSn$	Ω	0.7090	0.8435	0.704
Equivalent Rotor Leakage Reactance	$Xr1Sn$	Ω	3.938	2.418	4.310
Magnetization Reactance	Xm	Ω	66.70	63.921	68.0
Losses and Efficiency					
Losses of Stator Winding	P_{cus}	W	243.215	121.260	245.9
Losses of Rotor Cage	P_{cur}	W	137.417	163.130	136.3
Weight of Stator Tooth	G_{r1}	Kg	4.017	4.00721	3.94
Stator Teeth Fundamental Losses	p_{r1}	W	36.08	36.375	35.80
Weight of Yoke	G_{y1}	Kg	8.275	5.71537	5.71
Losses of Stator Back Iron Fundamental	p_{y1}	W	74,62	43.951	45.60
Fundamental Iron Losses	p_{iron1}	W	110.70	80.326	81.4
Weight of Rotor Teeth	G_{rr}	Kg	3.710	3.534	3.51
Tooth Flux Pulsation Core Loss	p_{irons}	W	7.2	6.929	5.81
Losses of Total Core	P_{ctotal}	W	117.9	87.255	87.2
Total Losses	PT	W	609.6	492.650	590.5

The time spent performing analytical calculations is too much, and calculation errors may occur due to the person performing the calculation. This study provides an advantage in terms of eliminating these negativities to a great extent. In addition, it is thought that the study will lead to new studies and contribute to researchers and engineers working on IM design.

5. CONCLUSION

In this study, an analytical tool, that could perform the calculations of three-phase squirrel cage IM, has been realized by using the Arduino Mega 2560 and the Nextion 7 inches touch screen, apart from previous studies in which these calculations have been performed by other various programming languages. In this study, a

portable, flexible, and minimum costly IM analytical calculation tool that works independently of the computer environment has been implemented with success. It is seen that analytical calculations results and the calculation results in the developed computer program tool are found in good agreement. This study aims to provide the opportunity to minimize the error rate in IM calculations, perform the preliminary design of the motor in less time, and achieve higher efficiency in motor design. The study ensures the users with the opportunity to make changes in the instant IM parameters and to see the change of the motor parameters depending on the change of these parameters. In the future, further studies will be done, to be made preliminary designs of these motors, by using the mathematical design parameters of synchronous and direct current motors.

DECLARATION OF ETHICAL STANDARDS

The authors of this article declare that the materials and methods used in this study do not require ethical committee permission and/or legal-special permission.

AUTHORS' CONTRIBUTIONS

Hasbi APAYDIN: He realized the electronic circuit design and software.

Necibe Füsün OYMAN SERTELLER: She wrote the manuscript and checked the accuracy of the results. Guidance and manuscript finalization.

Yüksel OĞUZ: He wrote the manuscript and checked the accuracy of the results. Guidance and manuscript finalization.

CONFLICT OF INTEREST

There is no conflict of interest in this study.

REFERENCES

- [1] Karakaya A., "Asenkron motorun modellenmesi ve modern denetim yöntemleri ile hız analizi", *Karaelmas Fen ve Mühendislik Dergisi*, 7(2): 497-502, (2017).
- [2] Kaya K. & Ünsal A., "Yapay Sinir Ağlarıyla Asenkron Motor Çoklu Arızalarının Tespiti ve Sınıflandırılması", *Politeknik Dergisi*, 25 (4) , 1687-1699, (2022).
- [3] Otkun O., "Scalar Speed Control of Induction Motors with Difference Frequency", *Politeknik Dergisi*, 23 (2) 267-276, (2020).
- [4] Khalghani S., "Analytical loss calculation tool for an induction motor", *Master's Thesis*, Lappeenranta-Lahti University of Technology LUT Lappeenranta, (2020).
- [5] Arslan S., Oy Akkaya S., Tarımer İ., "Investigation of Stator and Rotor Slits' Effects to the Torque and Efficiency of an Induction Motor", *TEM Journal*, Issue No: 1, Pages: 117- 125, (2017).
- [6] Arslan S., "Dalgaç Motorun Analitik, Sayısal, Performans Sonuçlarının Karşılaştırılması", *Düzce Üniversitesi Bilim ve Teknoloji Dergisi*, Volume 4, Pages 403 –415, (2016).
- [7] Gecer B., Tosun O., Apaydın H. and Serteller N. F. O., "Comparative analysis of SRM, BLDC and induction motor using ANSYS/Maxwell", **In 2021 International Conference on Electrical, Computer, Communications and Mechatronics Engineering (ICECCME)**, Mauritius,1-6, (2021).
- [8] Tarımer İ., "Bilgisayar Destekli Asenkron Motor Tasarımı", Gazi Üniversitesi Teknik Eğitim Fakültesi, *Politeknik Dergisi*, Cilt 8, Sayı 1, s.s. 19–24, Ankara, (2005).
- [9] Scutaru G., Negoita A. and Ionescu R. M., "Three-phase induction motor design software", **2010 IEEE International Conference on Automation, Quality and Testing, Robotics (AQTR)**, Cluj-Napoca, 1-4, (2010).
- [10] Aravind C.V., Grace I., Rozita T., Rajparthiban R., Rajprasad R. and Wong Y. V., "Universal computer aided design for electrical machines", **2012 IEEE 8th International Colloquium on Signal Processing and its Applications**, Malacca- Malaysia, 99-104, (2012).
- [11] Bhaskar L., "Simulink based model for determination of different design parameters of a three phase delta connected squirrel cage induction motor", *IOSR Journal of Electrical and Electronics Engineering (IOSR-JEEE)*, 7(4): 25-32, (2013).
- [12] Aguiar V. P. B., Pontes R. S. T. and Fernandes T. R., "Three-phase induction motor preliminar design assisted by cad software based on Brazilian standards", *Energy Efficiency in Motor Driven Systems (E-EMODS'2013)*, Rio de Janeiro, 1-11, (2013).
- [13] Zöhre B. and Akar M., "Matlab grafik arayüzü kullanılarak 3 fazlı asenkron motorların analitik modellenmesi", **1st International Mediterranean Science and Engineering Congress (IMSEC 2016)**, Adana-Türkiye, 3652-3659, (2016).
- [14] Deepa V., Bindu R., "Three phase induction motor design in windows programming platform", *International Journal of Engineering and Innovative Technology*, 3(1): 353-360, (2013).
- [15] Ike S. A., Enyong P. M. and Olowu T., "Programing the rewinding of a three-phase induction motor stator using interactive computer-aided design technique", *International Journal of Engineering & Technology*, 4(2): 350-357, (2015).
- [16] Somashekar B., "Design of three phase induction motor using matlab programming", *Int. J. Recent Innovation Trends Comput. Commun*, 3(8): 5188-5193, (2015).
- [17] Boldea I., Nasar S. A., "**The Induction Machine Design Handbook**", CRC Press, Boca Raton, 2010.
- [18] Upadhyay K. G., "**Design of electrical machines**", New Age International, New Delhi- India, (2011).
- [19] Gürdal O., "**Elektrik makinalarının tasarımı**", Bursa Orhangazi Üniversitesi Yayınları, Bursa, Türkiye, (2015).
- [20] Rahini V. and Nagarajans V. S., "**Electrical machine design**", First edition, Pearson, New Delhi- India, (2018).
- [21] Murthy K. V. M., "**Computer-aided design of electrical machines**", BS Publications, Hyderabad- India, (2008).
- [22] Yetgin A. G., Çanaköglü A. İ., Bekiroğlu K. N., Zorlu S., "Optimum Design and Performance Analysis of Three-Phase Induction Motor", **Eleventh International Conference on Electrical Machines, Drivers and Power Systems**, September 15–16, pp. 24–30, Sofia-Bulgaria, (2005).
- [23] https://nextion.tech/editor_guide/ (02/10/2022)
- [24] Yaşar E. "Bir tartım otomasyonunda, platform tipi yük hücrelerinin, S-tipi olarak kullanılması", *Avrupa Bilim ve Teknoloji Dergisi*, Ejosat Special Issue 2020 (ISMSIT): 221-227, (2020).
- [25] <https://store.arduino.cc/products/arduino-mega-2560-rev3> (02/10/2022)
- [26] Krajnc M., Kovač A., Zupančič A. and Šuštar, A., "Microcontroller-based ion meter application utilizing real-time data acquisition system", *Annals of Electrical and Electronic Engineering*, 2(3): 8-12, (2019).
- [27] Merhi N., Mohamad N., HajjMoussa G., ElSayed A., Bamashmos S H., Hamawy L. and Kassem A., "An intelligent infusion flow controlled syringe infusion pump", **31st International Conference on Microelectronics (ICM)**, Cairo- Egypt, (2019).

- [28] Aslam S., Hannan S., Sajjad U. and Zafar W., "Implementation of PID on PIC24F series microcontroller for speed control of a DC motor using MPLAB and Proteus", *Advances in Science and Technology Research Journal*, 10(31), 40-50, (2016).
- [29] Yetgin A. G., Turan M., Cevher B., Çanakođlu A. İ., Ayhan G. Ü. N., "Squirrel cage induction motor design and the effect of specific magnetic and electrical loading coefficient", *International Journal of Applied Mathematics Electronics and Computers*, 7(1), 1-8, (2019).

ERKEN GÖRÜNÜM